Electrical simulation and optimization of organic photovoltaic cells based PTB7:PC70BM

S. Bensenouci [a], K. Rahmoun [a], A. Aissat [b,c*]
[a]*Unit of Research on Materials and Renewable Energies, URMER, University of Telmcen AbouBakr Belkaid, BP 119, Tlemcen13000, Algeria*
[b]*University of Ahmed Draia Adrar, Algeria*
[c]*LATSI Laboratory, Faculty of Technology, University of Blida 1, Algeria*

This work presents electrical simulations and the optimization of the device structure ITO/PEDOT:PSS/PTB7:PC70BM/Al, using OghmaNano (Organic and hybrid Material Nano) software. The result analysis was given at different layer thickness and the best performance characteristics are obtained at 250 nm of the active layer. Then, the simulated results of different parameters such as charge carrier mobility, temperature and series resistance are investigated. Different structures of organic solar cells, the role of the interface layer used as a hole transport layer and the effect of electrodes are discussed. Finally, the energy level of the device is explained by the optical simulation and the optimized solar cell was proposed.

.

(Received December 9, 2023; Accepted March 15, 2024)

Keywords: Materials, Organic solar cells, PTB7: PCBM, Thickness, Detection

1. Introduction

Ternary organic solar cells (OSCs) have attracted wide attention in recent years. The first investigation of an OSC took place as early as 1959, the cell had a photovoltaic voltage of 200 mV with extremely low efficiency [1]. However, polymer-based photovoltaic devices exhibit low efficiencies compared to inorganic solar cells. Considered as a third generation of photovoltaic solar cells, organic solar cells have the potential to become serious competitors due to their many properties [2,3]. C.W. Tang [4] made one of the first organic solar cell in 1975 with a quite low efficiency. In 1979, Heeger, MacDiarmind and Shirakawa [5] have discovered that the conductivity of conjugated polymers can be increased by doping. Following to this contribution, they were awarded the Nobel Prize in chemistry in 2000. In 1986, the efficiency of the OCS reached is greater than 1% and electrical simulation achieved maximum efficiency of 13% [6,7]. An important development in organic PV came in the mid-1990s with the introduction of the bulk heterojunction (BHJ) device that has led to energy conversion efficiencies of about 5% [8]. In this device, an electron acceptor, generally a fullerene is used to improve morphology and processing, and a light absorbing polymer which is also a good hole carrier. In addition, each phase must be permanently connected for the transport of the respective charge carrier to separate electrodes [9]. So, the typical structure of an BHJ organic solar cell is constituted of a hole transport layer, generally poly (3,4-ethylenedioxythiophene):poly(styrene sulfonate) (PEDOT:PSS), is spin-coated on top of the anode. however, both hygroscopic and acidic with an associated reduction in device stability[10,11]. The active layer comprising the donor and the acceptor is sandwiched between the cathode and the hole transport layer (HTL) [12]. Using a bulk heterojunction based on the donor blends of Poly({4,8-bis[(2-ethylhexyl)oxy]benzo[1,2-*b*:4,5-b′]dithiophene-2,6-diyl}{3-fluoro-2-[(2-ethylhexyl)carbonyl]thieno[3,4-*b*]thiophenediyl}), (PTB7), and [6,6]-phenyl C71 butyric acid methyl ester (PC70BM) as active layer, the OSCs had great photovoltaic properties which are suitable for application in the light weight/flexible solar cell.

The active layer studied in this work, PTB7:PC70BM has achieved high performance power conversion efficiency in organic materials which has a potential lightweight, low cost, low band gap donor–acceptor polymer. This Donor blend polymer has shown an excellent charge

* Corresponding author: sakre23@yahoo.fr
https://doi.org/10.15251/JOR.2024.202.163

carrier life time, an absorption coefficient, and relatively a high carrier mobility [13]. However, the dependence of organic solar cell J-V characteristics at different active layer thickness is presented and the optimum active layer thickness is research to get the maximum efficiency using simulating software OghmaNano (Organic and hybrid Material Nano).

2. Theoretical analysis

OghmaNano is free general-purpose software for opto-electronic device simulation. This software has both electrical and optical model for accurate simulation [14,15]. The model solves all electrons, carrier continuity and drift-diffusion holes equations in the location space to describe the transport of charge carriers in the device. For the estimation of the electrostatic potential the Poisson's equation is also solves. In this model, the Shockley-Read-Hall (SRH) formalism is used to express recombination and carrier trapping, the distribution of trap states can be freely specified [16]. The basic equations used in this model are as followed.

$$\frac{\partial}{\partial x}\varepsilon_0.\varepsilon_r\frac{\partial \varphi}{\partial x} = \mathrm{q}.(n-p) \tag{1}$$

$$J_n = q\,\mu_e\,n\,\frac{\partial E_c}{\partial x} + q\,D_n\frac{\partial n}{\partial x} \tag{2}$$

$$J_p = q\,\mu_p\,p\,\frac{\partial E_v}{\partial x} - q\,D_p\frac{\partial p}{\partial x} \tag{3}$$

$$\frac{\partial J_n}{\partial x} = q\left(R_n - G + \frac{\partial\, n}{\partial x}\right) \tag{4}$$

$$\frac{\partial J_p}{\partial x} = -q\left(R_p - G + \frac{\partial\, p}{\partial t}\right) \tag{5}$$

where q is the elementary charge, ε_0, ε_r are the free and relative spacepermittivity respectively, n, p are the free electron and hole concentration, μ_e , μ_p are the electron and hole mobility, D_n , D_p are the electron and hole diffusion coefficient and R_n, R_p are the net recombination rate for electrons and holes. G is the free carrier generation rate.

In this model, there are two types of electrons (holes), free electrons (holes) and trapped electrons (holes). Free electrons (holes) have a finite mobility and trapped electrons (holes) cannot move at all and have a mobility of zero. To calculate the average mobility, the ratio of free to trapped carriers and multiply it by the free carrier mobility was taking as followed.

$$\mu_e(n) = \frac{\mu_{0,e} n_{free}}{n_{free} + n_{trap}} \tag{6}$$

$$\mu_p(n) = \frac{\mu_{0,p} p_{free}}{p_{free} + p_{trap}} \tag{7}$$

where $\mu_{0,e}$ and $\mu_{0,p}$are the electron/hole mobility edge, n_{free}, n_{trap} are the density of free and trapped electron, p_{free}, p_{trap} are the density of free and trapped hole respectively.

The bulk heterojunction (BHJ) solar cell simulated has a structure: ITO/PEDOT: PSS/PTB7:PC70BM/Al. This BHJ organic solar cell device contains four layers. The front contact transparent layer is ITO of thickness 100nm, the polymer contact layer or hole transport layer (HTL) is PEDOT: PSS of thickness 20nm,the metal back contact layer is Aluminum of thickness 100nm, the active layer is the mixture of fullerene PC70BM and the conjugated polymer PTB7 [17-19]. The thickness of the active layer is ranges from 50nm to 300nm by a step of 50. The efficiencies corresponding to each thickness are noted. The electrical parameters like open circuit voltage (V_{oc}), short circuit current density (J_{sc}), and fill factor (FF) are determined. We can add or remove any of these layers. According to the analysis, the thickness, the material and layer type can be changed. As shown in Table 1, electrical and optical parameters, used in this simulation, were selected from OghmaNano database and literature, at 300K as operating temperature.

Table 1. Active Layer Parameters set in simulation.

Parameters	
Electron trap density ($m^{-3}eV^{-1}$)	$3.8x10^{26}$
Hole trap density (m^{-3} eV^{-1})	$1.45\ x10^{25}$
Electron tail slope (eV)	0.04
Hole tail slope (eV)	0.06
Electron mobility ($m^2V^{-1}s$)	$2.48\ x10^{-7}$
Hole mobility ($m^2V^{-1}s$)	$2.48\ x10^{-7}$
Relative permittivity (au)	3.8
Number of traps bands	20
Free electron to trapped electron (m^{-2})	$2.5\ x10^{-20}$
Trapped electron to free hole (m^{-2})	$1.32\ x10^{-22}$
Trapped hole to free electron (m^{-2})	$4.67x10^{-26}$
Free hole to trapped hole (m^{-2})	$4.86\ x10^{22}$
Effective density of free electron states (m^{-3})	$1.28\ x10^{27}$
Effective density of free hole states (m^{-3})	$2.86x10^{25}$
Xi (eV)	3.8
E_g (eV)	1.1

3. Results and discussions

One of the different parameters which can increase the productivity in OSC is the layer thickness for a specific structure. In this research, the electrical simulation for different thickness is variable of the active layer wile all other parameters are the same. The structure of the OSC studies in this work modeled in Fig.1 and Table 2 presents the result obtained by OghmaNano simulation.

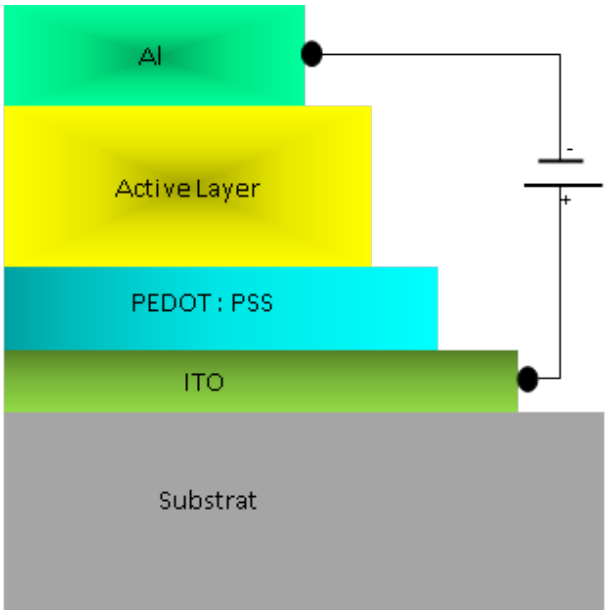

Fig.1. Typical structure modeling of an BHJ organic solar cell.

Table 2. Output parameters at different thickness of active layer.

Thickness (nm)	V_{oc}(V)	J_{sc} (mA/cm^2)	FF(%)	PCE (%)
50	0.620	-6.01	77.57	2.89
100	0.623	-10.82	75.43	5.08
150	0.609	-10.22	72.26	4.50
200	0.607	-11.68	68.29	4.84
250	0.605	-12.91	65.41	5.11
300	0.600	-12.49	62.56	4.69

The absorbance of PTB7: PC70BM is presented in Fig. 2. The device shows better absorption in visible spectra. Our results are compared with experimental [20] using FTO instead of ITO, the maximum of photons is absorbed in the range between 400 and 800 nm, and we notice that photons absorption is carried out in the active layer. The External Quantum Efficiency (EQE) calculated by OghmaNano software is shown in Fig.3; the EQE follows the absorption in the visible part of the spectrum, while they show an anti-symbatic behavior in the UV. This indicates that photons in the UV hardly contribute to the measured J_{sc}.

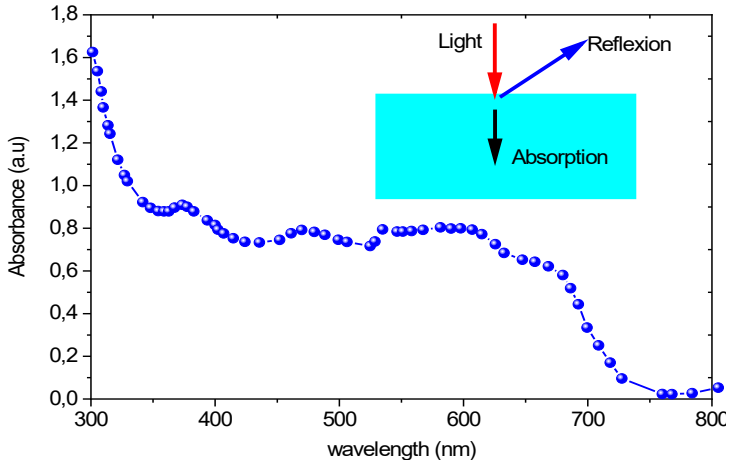

Fig.2. Absorbance of PTB7: PC70BM.

The J-V characteristics as a function of the thickness of the active layer are presented in Fig.4. In this analysis, the best J-V characteristic is obtained at 250 nm active layer thicknesses; the increase in thickness causes a drop in open circuit voltage due to the high recombination rate. When the thickness of the active layer increases the fill factor degrades, it is due to the increase of internal power depletion [21].

In order to validate our simulation on the solar cell performance, a device with PEDOT: PSS as HTM was simulated and compared with reported experimental [22-24] (table 3). This simulation results and those obtained experimentally by ref [22], are nearby with an efficiency difference ΔPCE=0.01.

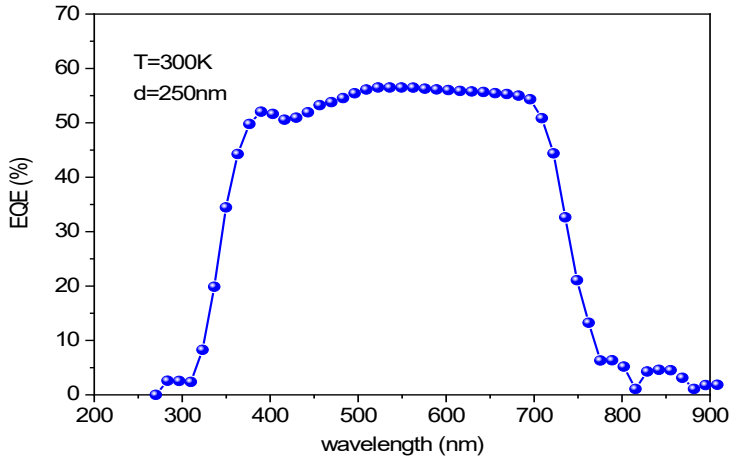

Fig.3. EQE spectra of ITO/PEDOT:PSS/PTB7 : PC70BM/Al d=250nm.

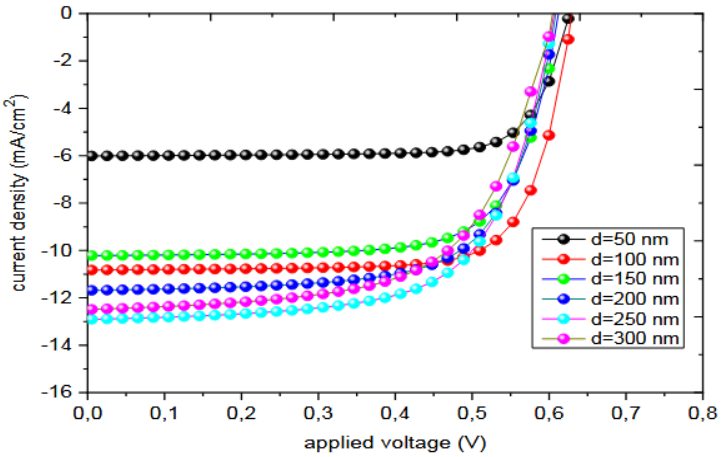

Fig. 4.J-V characteristic for different active layer thickness.

The J-V characteristics as a function of the thickness of the active layer are presented in Fig.4. In this analysis, the best J-V characteristic is obtained at 250 nm active layer thicknesses; the increase in thickness causes a drop in open circuit voltage due to the high recombination rate. When the thickness of the active layer increases the fill factor degrades, it is due to the increase of internal power depletion [21].

In order to validate our simulation on the solar cell performance, a device with PEDOT: PSS as HTM was simulated and compared with reported experimental [22-24] (table 3). This simulation results and those obtained experimentally by ref [22], are nearby with an efficiency difference ΔPCE=0.01.

Organic solar cells have two processes, extraction and recombination of charge carriers, these two processes are driven by the mobility of the charge carrier. increasing the mobility of charge carriers would have a positive effect on transport, and facilitating extraction, but on the other hand it increases bimolecular recombination [25]. At the donor-acceptor hetero junction, the photo-generated excitons are dissociated into electrons and holes. It is considered that the excitons dissociation probability is high enough that their concentration at the donor acceptor interface is zero. So, only the excitons generated with a distance of diffusion length from the hetero junction can contribute to the photo-current generation [26]. The effect of charge carrier mobility on V_{oc}, J_{sc}, FF and the power conversion efficiency (PCE) is shown in table 4. The dependence of solar

cell J-V characteristics on charge carrier mobility is presented in Fig.5. The best solar cell efficiencies are achieved at the mobility of $2.48x10^{-5}$ m^2/Vs.

Table 3. Simulated and measured solar cell J-V parameters.

	V_{oc}(V)	J_{sc} (mA/cm^2)	FF(%)	PCE (%)
ref [22]	0.77	- 9.70	40.00	2.97
ref [23]	0.58	- 14.10	62.40	5.10
ref [24]	0.67	- 15.94	67.20	7.18
This work	0.61	- 12.91	65.41	5.11

Table 4. Output parameters at different charge carrier mobility.

Mobility (m^2/Vs)	V_{oc}(V)	J_{sc}(mA/cm^2)	FF (%)	PCE (%)
$2.48\ x10^{-4}$	0.54	-13.09	78.01	5.55
$2.48\ x10^{-5}$	0.59	-13.09	78.22	6.01
$2.48\ x10^{-6}$	0.60	-13.08	76.10	5.99
$2.48\ x10^{-7}$	0.61	-12.91	65.41	5.11

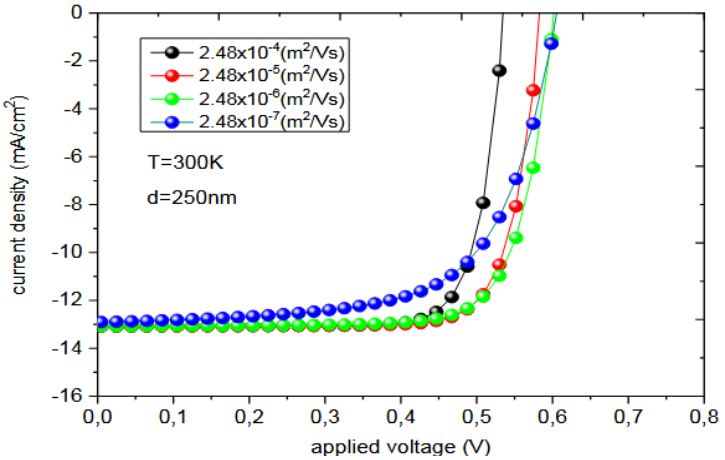

Fig. 5. Effect of charge carrier mobility on the J-V characteristic.

Table 5 presents the variation of V_{oc}, J_{sc}, FF and PCE of bends PTB7:PC70BM at different temperatures with a thickness of 250nm. Figure 6 (a,b) shows the temperature effect on the output parameters of the simulated solar cell. We report that increasing temperature causes variations in J_{sc}, V_{oc}, FF and PCE. The increase in temperature causes a decrease in open circuit voltage. On the other hand, the impact of the temperature on the current density is negligible (fig 6.a). Fig 6.b shows the effect of temperature on form factor and quantum efficiency. When the temperature varies from ΔT=60K, we had a relative increase in FF equal to 4.8% and a relative decrease in efficiency which is equal to 3.8%.

Table 5. Variation of power conversion efficiency of donor blends PTB7: PC70BM polymer at different temperatures.

Temperature (K)	V_{oc}(V)	J_{sc}(mA/cm^2)	FF(%)	PCE(%)
270	0.64	-12.78	63.31	5.17
285	0.62	-12.86	64.42	5.15
300	0.60	- 12.91	65.41	5.11
315	0.59	-12.95	65.99	5.03
330	0.57	-12.98	66.61	4.95
345	0.56	-13.00	66.82	4.83
360	0.54	-13.02	66.67	4.69
370	0.53	-13.03	66.88	4.60
380	0.52	-13.03	66.47	4.49

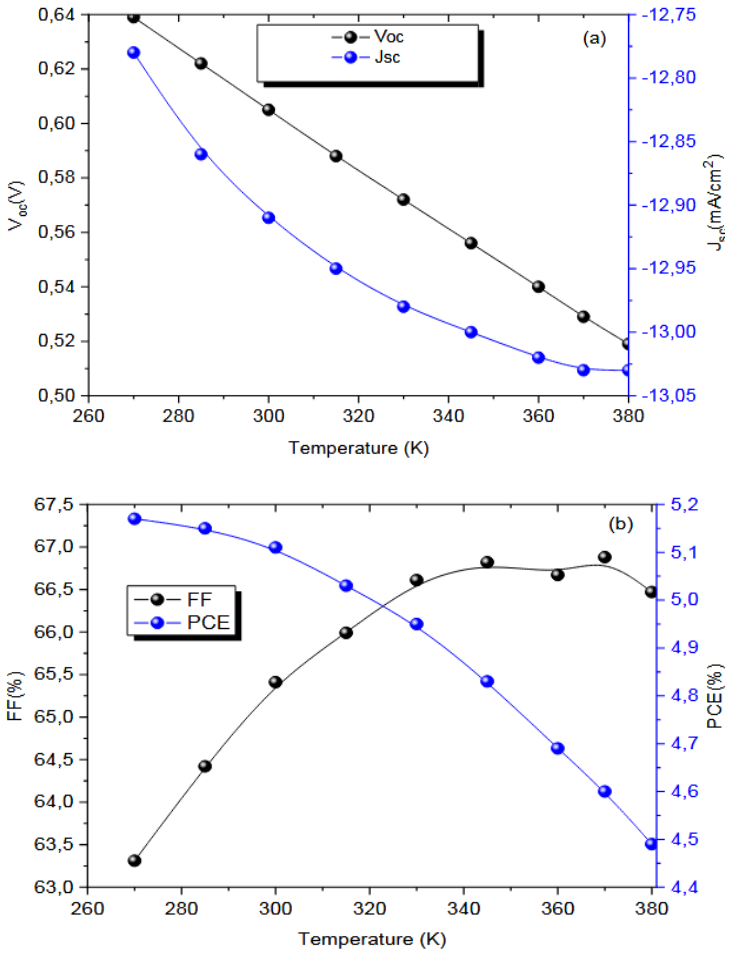

Fig.6. (a,b). The variation of a) Open-circuit voltage, short-circuits current density b) conversion efficiency, and fill factor (%) by varying the temperature.

Series resistance is one of the parameters governing the operation of an organic solar cell. Fig. 7 shows simulations of the effect of the variation of R_s on the J-V characteristics of the structure based on PTB7:PC70BM, present the effect of the series resistance on the characteristic parameters of the cell. The resistance series strongly affect the efficiency and the performance of the device through reduction of the fill factor. The best organic solar cells are those with low series resistance.

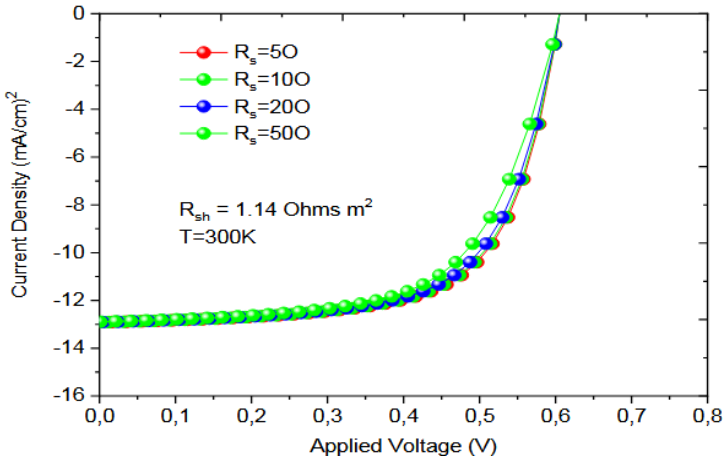

Fig.7. The effect of series resistance on J-V characteristics.

The integration of interfacial layers in organic photovoltaic cells remains a very delicate point in the development of organic photovoltaic cells. To realize the best configuration of these devices, it is a question of finding the right combination between: (i) the materials (interfaces with the cathode and the anode), (ii) the structure of the device (conventional or inverted), (iii) and manufacturing processes [27].

The interfacial layers were integrated into the organic devices to select the charges extracted from the active layer and to collect them at the electrodes according to their polarity [28]. The influence of the thickness of both PTB7:PC70BM and HTMs layers on the performance of the solar cell are shown in Fig.8 (a,b,c,d).

The influence of the PTB7:PC70BM thickness and HTM layers on the solar cell performance is shown in figure 8 (a,b,c). The increase in the thickness of the absorbent layer (d) induces a reduction in the open circuit voltage V_{oc} (Fig 8.a). Also, the increase in d causes a significant augment the short-circuit current density J_{sc} (fig 8.b). In figure 8.c the thickness d effect on the form factor FF has been simulated, we notice that the evolution of the thickness d decreases the fill factor (FF). In figure 8.d, the thickness d influence on the efficiency (PCE) has been taken into consideration. This simulation shows us when the thickness d varies from 50nm to 300nm the output parameters J_{sc}, V_{oc}, FF and PCE reach 12.76mA/cm^2, 0.6V, 62.48% and 4.76% respectively. We notice that this study allows us to optimize the structure of the solar cell presented. The optimized structure corresponds to d=250nm, with PCE= 5.17%.

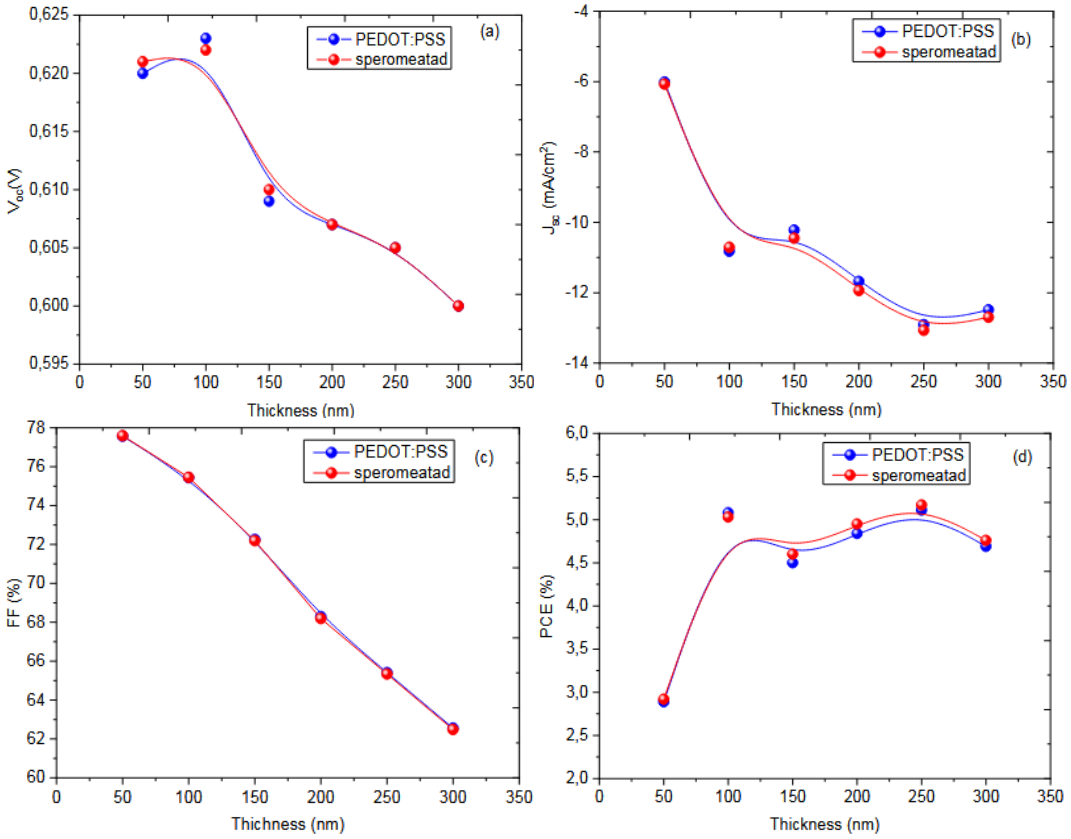

Fig.8. (a,b,c,d). a) Open-circuit voltage (V_{oc}), b) short-circuit current density (J_{sc}) , c) FF (%), d) PCE (%), via active layer thickness (nm) using PEDOT:PSS and Spiro-MeOTADas HTL.

Figure 9 illustrates the thickness (d) effect on the proposed solar cell efficiency for different thicknesses of the PEDOT layer (D). When the thickness d varies from 50 to 300nm we detect that the PCE varies from 3 to 4.70% with D=10nm, that is to say we had an increase in efficiency around 1.70%. For the optimal structure which corresponds to d=250nm and by varying the thickness D from 10 to 50nm the efficiency of the solar cell decreases from 5.15 to 4.76, that is to say we had losses of ΔPCE = 0.39% that is to say relative losses of 7.57%. So to optimize the performance of the proposed solar cell, we have to find a compromise between the two thicknesses d and D.

Figure 10 illustrates the variation of the solar cell efficiency as a function of the thickness of the active layer (d) for several thicknesses of the Spiro-MeOTAD layer (e) with D=20nm. By varying the thickness (e) from 10 to 50nm with D=20nm and d=250nm, the efficiency of the solar cell decreases from 15.15 to 4.97, under these conditions we had losses of ΔPCE=0.18%, this that is to say relative losses around 3.50%. This part of our work allows us to find a compromise between the thicknesses d, D and e in order to create a high-performance solar cell.

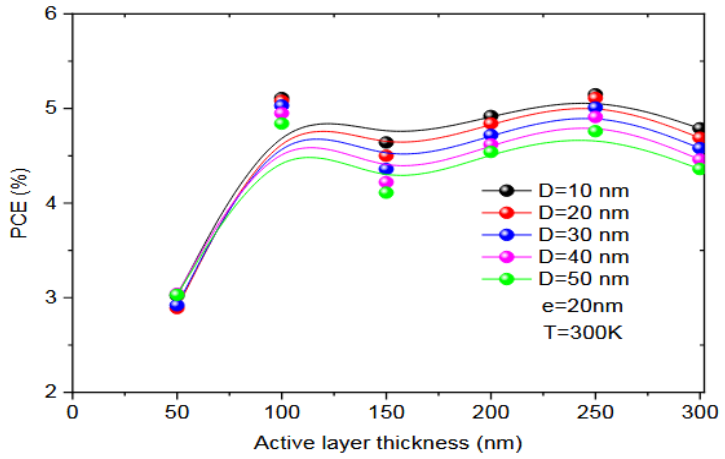

Fig.9. The thickness active layer (d) effect on the efficiency of the solar cell, for e=20nm, T=300K.

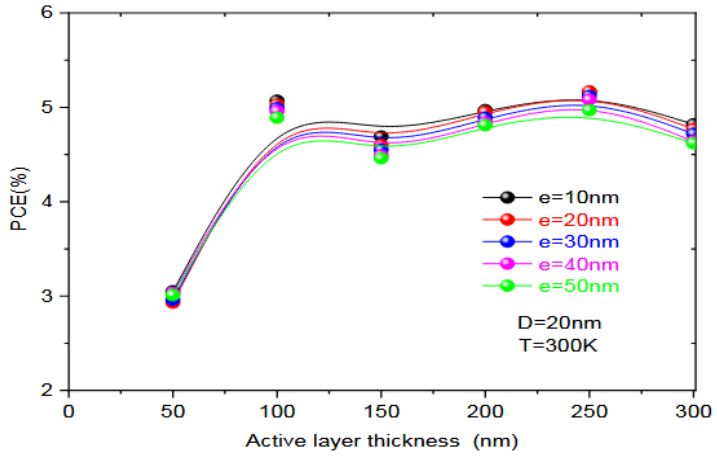

Fig.10. The thickness active layer (d) effect on the efficiency of the solar cell, for D=20nm, T=300K.

The spectral distribution of incident photons and the absorbed photons in the device shown in the Fig. 11, Fig.12 explain corresponding energy band gap of the intermediate layers of the device. OghmaNano will always perform an optical simulation if the light intensity is not set to zero, but it will not dump all the information it calculates to disk as this is too slow, therefore there is an optical simulation window to explore the optical performance of the device in more detail [29-31]. The emission input AM 1.5G solar spectrum was used in the optical device simulation, PTB7:PC70BM solar cell works in the visible region for the energy conversion.

The obtained results which allow showing the electrode nature influence on electric device performance are summarized in Table 6and the best results are obtained with FTO/Ag OPV cell. From the simulation of different parameters, the best performance is obtained for the structure FTO (100nm)/Spiro-MeOTAD (20nm)/PTB7:PC70BM (250nm)/Ag (100nm) with PCE of 5.20%. The J(V) characteristic of the optimized cell is given in Fig.13. The obtained optimum parameters V_{OC}, J_{SC}, FF and P_{max} of the solar cell are 0.60V, 13.14mA/cm^2, 65.3% and 7.95 watts respectively.

Table 6. Device performance with different electrode pairs.

Electrode	V_{oc} (V)	J_{sc} (mA/cm^2)	FF (%)	PCE (%)
ITO/Al	0.605	-13.07	65.34	5.17
FTO/Ag	0.605	-13.14	65.33	5.20
FTO/Au	0.605	-13.09	65.31	5.18

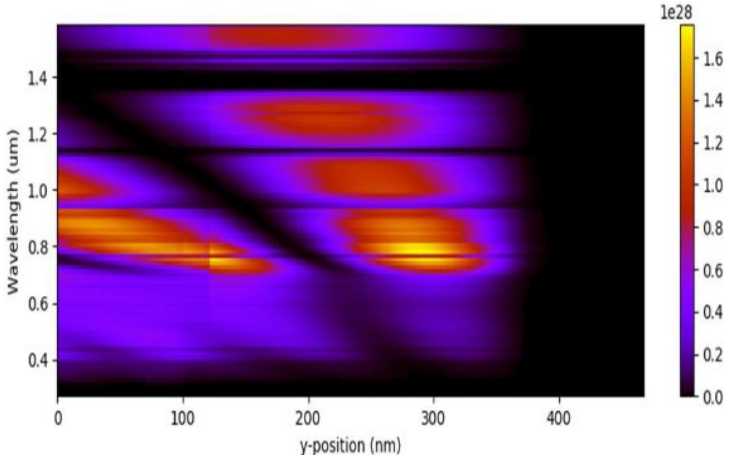

Fig. 11. Spectral distributions of incident photons of the donor blend PTB7:PC70BM polymer solar cell.

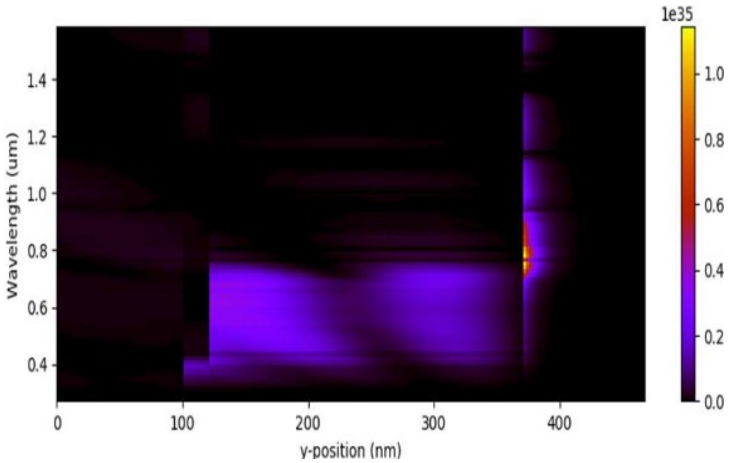

Fig. 12. Spectral distributions of absorbed photons of the donor blend PTB7:PC70BM polymer solar cell.

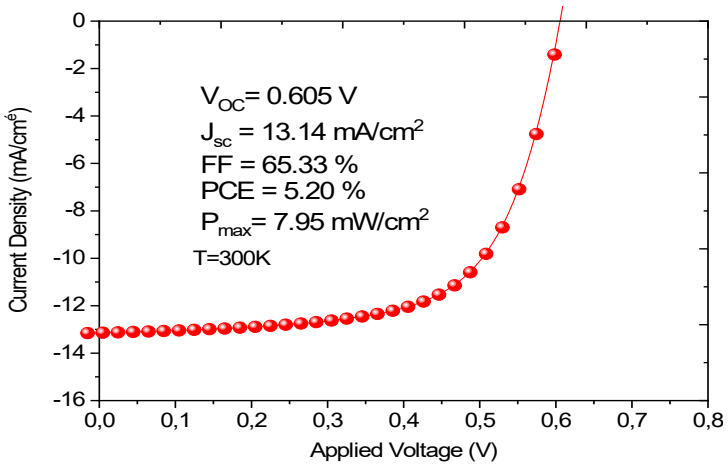

Fig. 13. Optimized Cell FTO/Spiro-MeOTAD(20nm)/PTB7:PC70BM(250nm)/Ag.

4. Conclusion

In this work, the electrical simulation and optimization of organic solar cells using OghmaNano software is presented with the device structureITO/PEDOT:PSS/PTB7:PC70BM/Al. The effect of the layer thickness and different electrical parameters such as charge carrier mobility, the temperature of the cell and series resistance are investigated. The best of J-V characteristic is obtained at 250 nm active layer thickness. The analysis of different structures of organic solar cells simulated and the role of the interface layer used as a hole transport layer and the effect of different electrodes allowed us to choose an optimized structure with suitable interface materials. The FTO/ Spiro-MeOTAD (20nm)/PTB7:PC70BM(250nm)/Ag optimized solar cell gave the following output parameters; J_{SC}=13.14 mA/cm^2, V_{OC} =0.60V, FF =65.3% and PCE=5.20%. Future work consists of improving the organic solar cells performances, using new organic materials based on inverted structures.

Acknowledgements

The authors declare that they have no known competing financial interests or personal relationships that could have appeared to influence the work reported in this paper.

References

[1] H. Kallmann, M. Pope, J. Chem. Phys., 30 (1959) 585-586;https://doi.org/10.1063/1.1729992
[2] E. Bundgaard, F. C. Krebs, Sol. Energy Mater. Sol. Cells, 91(11), (2007) 954-985; https://doi.org/10.1016/j.solmat.2007.01.015
[3] Y. Zhao, W. Liang, Chem. Soc. Rev., 41(3)(2012),1075-1087; https://doi.org/10.1039/C1CS15207F
[4] C. W. Tang, A. C. Albrecht, Nature, 254, 507-509(1975);https://doi.org/10.1038/254507a0
[5] I. B. Goldberg, H. R. Crowe, P. R. Newman, A. J. Heeger, A. G. MacDiarmid, J. Chem. Phys., 70(1979) 1132-1136; https://doi.org/10.1063/1.437613
[6] C. W. Tang, Appl. Phys. Lett., 48(1986)183-185; https://doi.org/10.1063/1.96937
[7] S. Sen, R. Islam, IOSR J. Appl. Phys. IOSR-JAP, 10 (2018)28-34
[8] J. M. J. Frchet, B. C. Thompson, Chem. Int. Ed. 2008, 47, 58-77; https://doi.org/10.1002/anie.200702506
[9] J. Bisquert, G. Garcia-Belmonte, J. Phys. Chem. Lett.. 2, 2011, 1950-1964;

https://doi.org/10.1021/jz2004864
[10] K. Sun, B. Zhao, V. Murugesan, A. Kumar, K. Zeng, J. Subbiah, W. H. Wallace, J. David, Ouyang, J. Mater. Chem.22 (2012), 24155-24165; https://doi.org/10.1039/c2jm35221d
[11] J.-T. Chen, C.-S. Hsu, Polym. Chem. 2,(2011) 2707-2722;https://doi.org/10.1039/c1py00275a
[12] M. Ghorab, A. Fattah, M. Joodaki, Optik 267 (2022) 169730;https://doi.org/10.1016/j.ijleo.2022.169730
[13] A. K. Mishra, R. K. Shukla, Mater. Today Proc.. 46 (2021) 2288-2293; https://doi.org/10.1016/j.matpr.2021.04.084
[14] M. Sittirak, J. Ponrat, K. Thubthong, P. Kumnorkaew, J. Lek-Uthai, Y. Infahsaeng, J. Phys. Conf. Ser.1380 (2019) 012146; https://doi.org/10.1088/1742-6596/1380/1/012146
[15] A. Hima,A. K. LeKhouimes, A. Rezzoug, M. BenYahkem, A. Khechekhouche I. Kemerchou, Int. J. Energ. 4 (2019) 56-59; https://doi.org/10.47238/ijeca.v4i1.92
[16] R. C. I. MacKenzie, T. Kirchartz, G. F. A. Dibb, J. Nelson, J. Phys. Chem. C. 115 (2011)9806-9813; https://doi.org/10.1021/jp200234m
[17] Z. Jin, D. Gehrig, C. Dyer-Smith, E. J. Heilweil, F. Laquai, M. Bonn, D. Turchinovich, J. Phys. Chem. Lett.5 (2014) 3662-3668; https://doi.org/10.1021/jz501890n
[18] Z. Li, G. Lakhwani, N. C. Greenham, C. R. McNeill, J. Appl. Phys. 114(2013) 034502; https://doi.org/10.1063/1.4813612
[19] L. Lu, Z. Luo, T. Xu, L. Yu, Nano Lett., 13(2013) 59-64;https://doi.org/10.1021/nl3034398
[19] I. Etxebarria, A. Guerrero, J. Albero, G. Garcia-Belmonte, E. Palomares, R. Pacios, Org. Electron. 15(2014) 2756-2762; https://doi.org/10.1016/j.orgel.2014.08.008
[20]J. C. Gomez, G.I. G. Alvarado, M. Pal , S.A. M. Hernandez , F. D. M. Flores, A. S. Domínguez, R. A. Devi, J. S. Cruz, Optik 247 (2021) 167961;https://doi.org/10.1016/j.ijleo.2021.167961
[21] K. Jahangir, G. A. Nowsherwan, S. S. Hussain, S. Riaz, S. Naseem, ICRRD J. Int. Res. J. Scopus Stand. Acad. Res. J.2 (2021) 131-140;https://doi.org/10.53272/icrrd.v2i3.4
[22] G. T. Mola, W. E. Dlamini, S. O. Oseni, J Mater Sci: Mater Electron.27(2016) 11628-11633; https://doi.org/10.1007/s10854-016-5295-6
[23] L. Lu, L. Yu, Adv. Mater.26 (2014) 4413-4430;https://doi.org/10.1002/adma.201400384
[24] C. T. Howells, K. Marbou, H. Kim, K. J. Lee, B. Heinrich, S. J. Kim, A. Nakao, T. Aoyama, S. Furukawa, J. H. Kim, E. Kim, F. Mathevet, S. Mery, I. D.W. Samuel, A. Al Ghaferi, M. S. Dahlem, M. Uchiyama, S. Y. Kim, J. W. Wu, J. C. Ribierre, C. Adachi, D. W. Kim, P. André, Journal of Materials Chemistry A,4 (2016)42521-4253;https://doi.org/10.1039/C6TA00677A
[25] N. Singh, A. Chaudhary, S. Saxena, M. Saxena, N. Rastogi, IOSR Journal of Applied Physics, 9(2017) 01-04; https://doi.org/10.9790/4861-0902020104
[26] N. Rastogi, N. Singh, S. Saxena, Universal Journal of Materials Science, 5 (2017) 83-87; https://doi.org/10.13189/ujms.2017.050401
[27] Y. Jouane, Theses, Université Louis Pasteur - Strasbourg France, 2012.
[28] Z.Yin, J. Wei, Q. Zheng, Adv.Sci. 3, (2016), 1500362
[29] L. Sims, U. Hörmann, R. Hanfland, R. C. I. MacKenzie, F. R. Kogler, R. Steim P. Schilinsky, Org. Electron., 15 (2014) 2862-2867;https://doi.org/10.1016/j.orgel.2014.08.010
[30] Y. Gao, R. C. I. MacKenzie, Y. Liu, B. Xu, P. H. M. van Loosdrecht, W. Tian, Adv. Mater. Interfaces 2 (2015) 1400555; https://doi.org/10.1002/admi.201400555
[31] Y. Liu, R.C.I. MacKenzie, B. Xu, Y. Gao, M. Gimeno-Fabra, D. Grant, P. H. M. van Loosdrecht, T. Wenjing, J. Mater. Chem. C. 3 (2015) 12260-12266; https://doi.org/10.1039/C5TC02678D